

## MODELLING CHEMICAL EQUILIBRIUM PARTITIONING WITH THE GEMS-PSI CODE

D. Kulik, U. Berner, E. Curti

*Sorption, co-precipitation and re-crystallisation are important retention processes for dissolved contaminants (radionuclides) migrating through the sub-surface. The retention of elements is usually measured by empirical partition coefficients ( $K_d$ ), which vary in response to many factors: temperature, solid/liquid ratio, total contaminant loading, water composition, host-mineral composition, etc. The  $K_d$  values can be predicted for in-situ conditions from thermodynamic modelling of solid solution, aqueous solution or sorption equilibria, provided that stoichiometry, thermodynamic stability and mixing properties of the pure components are known (Example 1). Unknown thermodynamic properties can be retrieved from experimental  $K_d$  values using inverse modelling techniques (Example 2). An efficient, advanced tool for performing both tasks is the Gibbs Energy Minimization (GEM) approach, implemented in the user-friendly GEM-Selector (GEMS) program package, which includes the Nagra-PSI chemical thermodynamic database. The package is being further developed at PSI and used extensively in studies relating to nuclear waste disposal.*

### 1 WHAT IS EQUILIBRIUM PARTITIONING?

The term Equilibrium Partitioning denotes the (equilibrium) distribution of a chemical element (M) between two phases of variable composition – usually a mineral solid solution and an aqueous solution. A measurable quantity called *partition coefficient* is defined as:

$$K_d = \frac{[M]_S}{[M]_{AQ}} \quad (1)$$

Here,  $[M]_S$  is the concentration of M in the solid phase (S), and  $[M]_{AQ}$  is that in the aqueous solution (AQ). Except for very simple systems,  $K_d$  is usually a complex function of temperature  $T$ , solid/liquid ratio  $s/l$ , total element inventory  $M_{TOT}$ , aqueous composition (pH, Eh, ionic strength  $I$ , concentrations of complexing ligands  $[L]$ ), and host-mineral composition. Measured  $K_d$  values may also be influenced by sorption or precipitation kinetics. Thus,  $K_d$  is a conditional constant, i.e. it applies only to specific experimental conditions, and cannot be generalised. All this makes the empirical  $K_d$  value not the perfect choice for long-term predictions of trace element distributions; hence, more fundamental theoretical approaches are necessary.

Calculations of aqueous speciation and saturation indices of pure solids, like  $MCO_3$  and  $MOOH$ , can easily be performed using widespread computer models, such as PHREEQC [1], but they are not always helpful in understanding the relationships between  $K_d$  and system variables. Experimental  $K_d$  values for trace metals are often significantly different from theoretical partition coefficients obtained from solubility products of pure solids. This fact indicates that the aqueous concentration of metals is not always controlled by simple, pure solid equilibria, but rather by other retention mechanisms involving the host mineral phases – namely, sorption, re-crystallisation or co-precipitation. In all these cases, the concept of a fixed thermodynamic solubility fails because of *variable compositions of both solid and aqueous*

phases; dissolved  $[M]_{AQ}$  would no longer be the solubility in the classical sense of the word. Attempts to use variable solubility products depending on the composition of aqueous solution, or of a mixed solid, were disappointing, because the law of mass-action alone does not seem to be sufficient for solving the solid-solution aqueous-solution (SSAS) equilibria. Some supporting tools, like the Lippmann functions and diagrams [2,3], can help in binary systems, but not in higher-order systems [4], or if two or more solid solutions are involved.

Hence, for an adequate thermodynamic description of partitioning, it is necessary to go back to the more basic concept introduced by Gibbs, which states that the chemical potential of M is the same in all co-existing phases at equilibrium. The equilibrium state is determined by finding mole amounts of all chemical species in all phases such that the total Gibbs free energy of the system is minimal at the given state variables (temperature  $T$ , pressure  $P$ , bulk mole composition vector  $\mathbf{b}$ ). In this approach, a variable-composition phase is fully defined by stoichiometry and mole amounts of its end-members (components, species), which need not necessarily exist as pure substances. The stability of each end-member is given by its standard molar Gibbs free energy  $G^\circ$  of formation from chemical elements. A deviation from ideal mixing with other end-members (excess partial molar Gibbs energy,  $\bar{G}_{real} - \bar{G}_{ideal} = \bar{G}^{Ex} = RT \ln \gamma$ ) is described by the activity coefficient  $\gamma$ , a function of the actual phase composition.

### 2 METHODS OF SPECIATION CALCULATIONS

Two numerical methods of chemical thermodynamic modelling can be applied to heterogeneous aquatic systems: (i) Law-of-Mass-Action — Reaction Stoichiometry (LMA), and (ii) direct Gibbs Energy Minimisation (GEM). The LMA approach is common, and available in many speciation codes, such as PHREEQC [1], MINEQL [5] or EQ3/6 [6], some equipped with data

bases of thermodynamic constants valid up to hydrothermal conditions. The GEM approach, represented by codes such as ChemSage/FactSage [7,8], GIBBS/Hch [9], Selektor [10,11] or GEMS-PSI, is less common, but is becoming increasingly popular.

## 2.1 LMA

The LMA approach is extensively described in textbooks [12,13]. Briefly, it requires no thermodynamic data for the “master” species (usually aqueous ions), but only the  $\log K$  of formation of the “product” species at the  $P, T$  of interest.

To find the “speciation”, i.e. equilibrium concentrations of aqueous ions or complexes, surface species and solids included, LMA codes usually employ the Newton-Raphson method. This iteratively solves a system of material balance equations, with non-linear boundary conditions being in the form of mass action equations for product species [1]. The LMA algorithm actually minimises the material balance residuals to very good precision:  $10^{-18} \div 10^{-21}$  molal, relative to the master species.

Unfortunately, the LMA algorithm in its common form has some serious limitations in setting up and solving *multi-phase* models involving partitioning. Namely: (i) only one variable composition phase is tolerated in the mass balance (usually the aqueous electrolyte) — all other phases (pure solids, solid solutions) must be taken at fixed compositions, and with constant solubility products; (ii) usually, stable solids must be known in advance, in order to be included into the mass balance; (iii) surface complexes are treated in the same way as aqueous complexes, but are subject to additional balance constraints on total amount of surface sites and, optionally, to electrostatic correction terms; and (iv) redox couples must be set at input by assigning different redox states of the same element, either by separate mass-balance constraints (e.g. for  $\text{Fe}^{\text{II}}$  and  $\text{Fe}^{\text{III}}$ ), or by the input  $\text{pe}$  or  $\text{Eh}$  of the aqueous solution.

## 2.2 GEM

The GEM approach is based on a mass balance for the entire system, which is set up by specifying the total amounts of chemical elements and a charge balance only. These elements and electric charge are called “Independent Components” (ICs, belonging to the set  $N$ ). All chemical species, in all phases, are called “Dependent Components” (DCs, belonging to the set  $L$ ), since their stoichiometries can be built from ICs. To some extent, ICs can be compared with LMA “master species”, and DCs with the “product species”. A significant difference between them lies in the explicit definition of the thermodynamic *phases* (belonging to the set  $\Phi$ , each including one or more DCs and additional properties, such as the specific surface area) in the GEM system formulation. Each DC is provided at input with its elemental stoichiometry, and a value of the standard molar (or partial molal) Gibbs energy  $G^\circ$ , which is taken from

the database and corrected to the  $P, T$  of interest, if necessary.

In the GEM method, the activities and concentrations of the DCs are treated separately for each phase, taking into account appropriate standard/reference states and activity coefficients. The equilibrium assemblage conforming to the Gibbs phase rule can be (in principle) selected automatically from a large list of stoichiometrically possible phases. The equilibrium partitioning in a multiphase system, including for example an aqueous solution, a gas mixture, one or several solid solutions, and, optionally, sorption phases, is computed simultaneously for all phases in a straightforward way. The GEM “Interior Points Method” (IPM) algorithm [10,11] does all this because, in addition to the *speciation vector*  $\mathbf{x}$  (mole amounts of DCs – the *primal solution*), it computes simultaneously a complementary *dual solution vector*  $\mathbf{u}$  (holding equilibrium chemical potentials of ICs at the state of interest). As shown below, the power of GEM IPM lies in comparing the DC chemical potentials obtained from primal  $\mathbf{x}$  and dual  $\mathbf{u}$  vectors, wherever possible.

## 3 GEM CONVEX PROGRAMMING METHOD

### 3.1 Mathematical Formulation

The goal of GEM is to find a vector of the DC mole amounts,  $\mathbf{x} = \{x_j, j \in L\}$ , such that:

$$G(\mathbf{x}) \Rightarrow \min, \text{ subject to } \mathbf{A}\mathbf{x} = \mathbf{b} \quad (2)$$

where  $\mathbf{A} = \{a_{ij}, i \in N, j \in L\}$  is a matrix of formula stoichiometry coefficients of the  $i$ -th IC in the  $j$ -th DC,  $\mathbf{b} = \{b_i, i \in N\}$  is the input vector of total mole amounts of IC, and  $G(\mathbf{x})$  is the total Gibbs energy function of the whole system:

$$G(\mathbf{x}) = \sum_k \sum_j x_j v_j, \quad j \in L_k, k \in \Phi \quad (3)$$

In Eqn. (3),  $L_k$  is a subset of DC in the  $k$ -th phase, and  $v_j$  stands for the dimensionless chemical potential of the  $j$ -th DC:

$$v_j = \frac{G_{j,T}^\circ}{RT} + \ln C_j + \ln \gamma_j + C_F + \text{const}, \quad j \in L_k \quad (4)$$

where  $G_{j,T}^\circ$  is the standard molar Gibbs energy,  $R = 8.3145 \text{ J}\cdot\text{K}^{-1}\cdot\text{mol}^{-1}$  is the universal gas constant,  $T$  is temperature (K),  $C_j = f(x_j)$  is concentration,  $\gamma_j$  is the activity coefficient of the  $j$ -th DC in its respective phase,  $C_F$  stands for the Coulombic term (for charged surface complexes), and *const* converts from the practical to the rational (mole fraction) standard-state concentration scale. The more detailed theory, with expressions for  $v_j$  in aqueous, gaseous, solid/liquid solution and sorption phases, can be found in [10,11,14].

The IPM is a non-linear minimisation algorithm specifically developed to solve chemical equilibrium

problems involving many potential single- and multi-component phases. This “engine” of the Selektor modelling codes [15] finds simultaneously two vectors, the primal  $\hat{\mathbf{x}}$  and the dual  $\hat{\mathbf{u}}$  optimal solutions of the problem (2), by checking the *Karpov-Kuhn-Tucker* (*KKT*) necessary and sufficient conditions for  $G(\mathbf{x})$  to be minimum [10]. The *KKT* conditions can be written in the integrated vector-matrix form for the case of complete equilibrium as:

$$\begin{aligned} \mathbf{v} - \mathbf{A}^T \hat{\mathbf{u}} &\geq 0; \\ \mathbf{A} \hat{\mathbf{x}} &= \mathbf{b}; \quad \hat{\mathbf{x}} \geq 0; \\ \hat{\mathbf{x}}^T (\mathbf{v} - \mathbf{A}^T \hat{\mathbf{u}}) &= 0 \end{aligned} \quad (5)$$

where the superscript  $T$  represents the transpose operator. When rewritten with indices for a  $j$ -th species:

$$v_j - \sum_i a_{ij} u_i \geq 0, \quad i \in N \quad (6)$$

the first *KKT* condition (Eqn. 5) implies that, for any  $j$ -th species (DC) present at equilibrium concentration  $C_j$  in its phase, the *primal* chemical potential  $v_j$  (calculated from the equilibrium mole amount  $\hat{x}_j$  and the standard molar Gibbs energy  $G_j^o$  according to Eqn. 4) is equal to a *dual* (stoichiometric) chemical potential

$$\eta_j = \sum_i a_{ij} u_i, \quad i \in N \quad (7)$$

Hence, dual solution values  $u_i$  are *chemical potentials of independent components* (IC) at the equilibrium state of interest, i.e. at given  $P$ ,  $T$  and  $\mathbf{b}$  of the system.

The last “orthogonality” *KKT* condition in Eqn. 5 helps to zero off molar amounts  $\hat{x}_j$  of unstable species for which the first *KKT* condition (Eqn. 6) cannot be met, because of either the mass-balance (second condition) or non-negativity (third condition) constraints. It is, in fact, this last condition that gives rise to the name “Selektor”, because the orthogonality constraint enables the algorithm to “switch off” unstable species and phases.

The *KKT* conditions were also extended for the case for which the sought-after mole amounts  $\hat{x}_j$  of some DCs are subject to the metastability constraints [11]. This makes it possible to use the GEM IPM algorithm for simulating various kinetically-dependent processes, such as sequences of partial equilibrium states.

Overall, the *KKT* conditions, and the related vector-matrix notation, can be regarded as a very condensed and precise representation of equilibria in isobaric-isothermal, heterogeneous, multiphase systems of any complexity and size. A large number of multi-component phases can be included simultaneously in the initial approximation. Such equilibria can be found using the IPM algorithm, as long as the internally-consistent, standard-state molar properties of the DCs at the  $P, T$  of interest, and the equations for the calculation of the activity coefficients in the phases,

are all provided. In many cases, the inconsistent input stoichiometries and thermodynamic data can be detected automatically.

### 3.2 Dual Thermodynamics

For any species, in any phase present at equilibrium, Eqns. (4,6) can be combined into a *DualTh* (“dual thermodynamic”) equation that compares “dual” and “primal” DC chemical potentials as  $\eta_j = v_j$ , or

$$\sum_i a_{ij} u_i = \frac{G_{j,T}^o}{RT} + \text{const} + \ln C_j + \ln \gamma_j + C_F \quad (8)$$

The difference  $\eta_j - G_{j,T}^o/RT$  defines the *activity* of the  $j$ -th DC. Hence, the activity of *any* chemical species can be retrieved from its  $G_{j,T}^o$  value, the chemical formula, and the dual solution vector  $\mathbf{u}$ . Indeed, Eqn. (8) is used within the GEM-Selektor code to compute: (i) activities of gases, aqueous, solid-solution and surface species; (ii) saturation indices for single-component condensed phases; and (iii) activity functions such as pH, pe and Eh. For instance, in aquatic systems, Eh (in Volts) is computed [11] according to:

$$\text{Eh} = \frac{RTu_e}{F} = 0.000086 \cdot T \cdot u_e \quad (9)$$

where  $u_e$  is the dual chemical potential relating to the charge balance constraint, and  $F$  is Faraday’s constant. Likewise, pH is computed *without* using the molality or the activity coefficient of the  $\text{H}^+$  ion:

$$\text{pH} = -0.4343 \cdot (u_H + u_e) \quad (10)$$

in which the coefficient -0.4343 derives from the conversion  $\ln$  to inverse  $\log_{10}$  scale. Hence, the equilibrium values of redox potential and pH can be found in a simple and general way, without applying more specific and complex electrochemical relationships.

Another application of Eqn. (8) is gaining more importance in “inverse modelling”, which is aimed at retrieving of thermodynamic data from the experimental equilibrium partitioning data. The idea [11] of such calculations, which can be termed “dual-thermodynamic” (*DualTh*), is quite simple. Suppose that bulk compositions, for example of an aqueous electrolyte, and the equilibrated solid solution phase have been measured. Then, the  $\mathbf{u}$  vector of dual potentials  $u_i$  can be computed using GEM IPM by modelling equilibrium speciation in the aqueous phase, but *without* considering the solid solution phase of interest in the mass balance. Next,  $u_i$  values can be used along with the concentration  $C_j$  (calculated from the measured bulk composition of solid solution phase and the  $j$ -th end-member stoichiometry) to find one unknown parameter on the right-hand side of Eqn. (8).

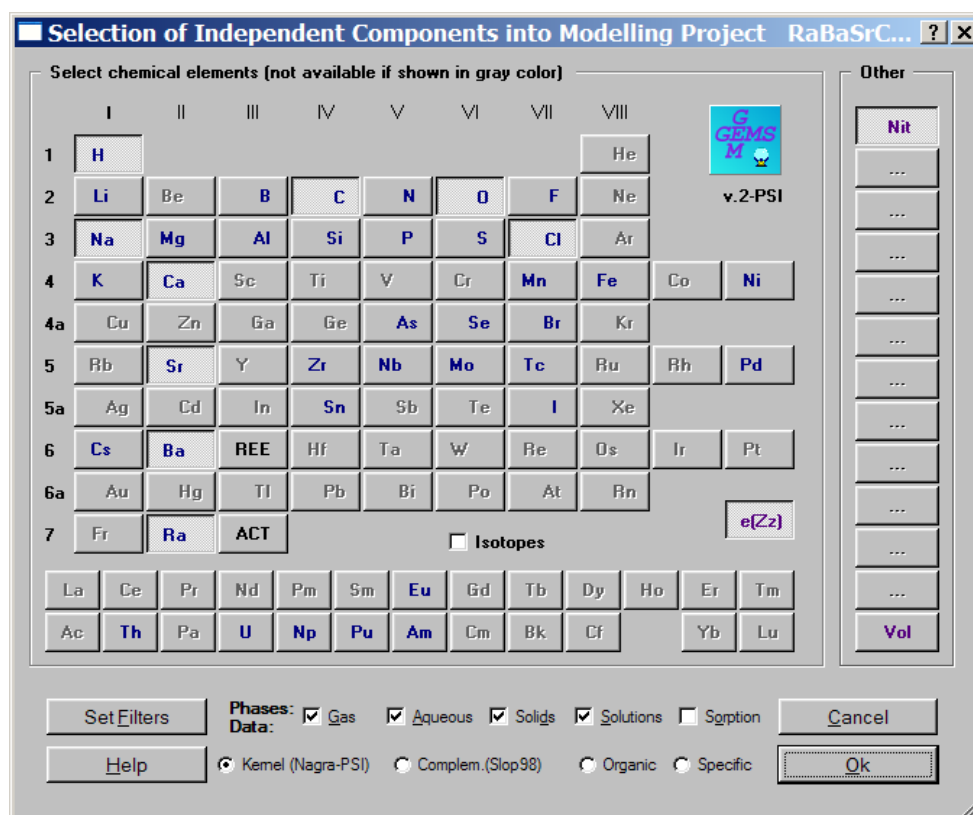


Fig. 1: Screen image of GEMS dialogue for selecting independent components to create a new modelling project.

If the  $G_{j,T}^o$  value is known, the activity coefficient  $\gamma_j$  of the  $j$ -th end-member can be found, and converted into parameter(s) of the chosen mixing model [4]. Otherwise, the unknown  $G_{j,T}^o$  value can be determined for a specific mixing model [16]; see also Example 2 below. If several experimental points at different compositions are available, then an unlimited number of alternative end-member stoichiometries can be compared, leading to identification of an “optimal” stoichiometry, including a  $G_{j,T}^o$  estimate and its uncertainty. This technique can also be helpful in the planning of new co-precipitation experiments, and, at a later stage, in interpreting their results.

#### 4 GEM-SELEKTOR V.2-PSI PACKAGE

GEM-Selektor (GEMS) is a user-friendly *geochemical modelling package* in which the GEM method is implemented. In particular, GEMS-PSI inherits the IPM non-linear minimisation algorithm from *Selektor* codes developed since 1973 in Russia, and since 1991 internationally.

The GEMS package, written in C/C++, combines the high-precision IPM-2 module [15] with software tools for setting up and running the user’s modelling projects, managing built-in thermodynamic databases, and re-calculating thermodynamic data. All data and controls are accessible through a

modern graphical user interface (GUI), based on the cross-platform Qt® toolkit [17], thanks to which the code compiles on Windows®, Linux®, Mac OS X, and other platforms. The GEMS-PSI package (at present, Windows, and soon Linux, versions) can be downloaded free of charge from the following web page: <http://les.web.psi.ch/Software/GEMS-PSI>. The package has been made available to a broad research community in the hope of collecting user feedback, and thereby to continuously improve the code and documentation.

The setup of new modelling projects, phases and species is facilitated by the GEMS GUI (Fig. 1), which also includes a run-time help browser. The input standard-state thermodynamic data are automatically corrected to the temperatures and pressures of interest using well-established techniques appropriate for solids, gases, aqueous and surface species. In addition, GEMS can also simulate various irreversible mass-transfer processes, such as titrations, mixing, weathering or sequential reactors, from the principles of local and partial equilibrium. Results of such “process simulations” are stored in the project data-base, and can easily be tabulated or plotted at run-time (Fig. 2), or exported to text files.

##### 4.1 GEM-Selektor IPM-2 Module

The sensitivity (minimum mole amount of IC) and precision (maximum mass-balance residual) of the original IPM algorithm [10] were not always sufficient

for modelling systems with trace radionuclide concentrations. Hence, a collaboration project was undertaken in 2001-2002, which resulted in an improved IPM-2 module [15]. The sensitivity and precision parameters achieved in IPM-2 are usually as good as those in LMA codes. The precision that can actually be attained depends on the internal consistency of the input thermodynamic data, and to some extent also on the bulk composition (buffering capacity) of the chemical system. The IPM-2 module also converges well with highly non-ideal systems, including solid solutions, or electrostatic surface complexation on heterogeneous mineral-water interfaces.

#### 4.2 Thermodynamic Database

The GEMS package includes two built-in *chemical thermodynamic databases*, compiled from Nagra/PSI 01/01 [18] and SUPCRT92-98 [19] data sets. The necessary data is automatically selected, and then copied into the *modelling project database*, when the user sets up a new modelling project (see Fig. 1). There, the data will become immediately available for the calculation of the equilibrium states, after providing a “recipe”: i.e. the bulk composition of the system, optionally including the non-ideality and metastability parameters. Later, the user can easily extend the project database with new dependent components and phases, as well as replace some records with his/her own input thermodynamic data, if needed and justified. Only the Nagra/PSI 01/01 database is officially supported by PSI/LES [20]; thermodynamic data from other sources can be involved at the user’s discretion only.

To extend the range of applications of GEMS-PSI beyond low-temperature aquatic systems relevant to nuclear waste disposal, a “third-party database” collaboration strategy has been developed. In such a collaboration, an external research team maintains a web page, with a specific thermodynamic database, in GEMS format. Anyone can download it, and then use it as a “plug-in” in the already installed GEMS-PSI package, or instead of the original built-in database. In this case, the only task required of the GEMS-PSI Development Team is to make sure that the third-party database has been correctly imported in the GEMS format, and that all calculations pertinent to that database are correctly performed by the GEMS code.

#### 4.3 Graphical User Interface (GUI)

The user-friendly GUI is essential in improving the quality and acceptability of the interpretation of the modelling results, and in saving the researcher’s working time. The GEMS GUI, together with database management modules and screen forms, tool tips, runtime help browser and online documentation, makes the set-up or modification of modelling problems quick and easy. Almost all modelling projects eventually need to be extended to include new phases and chemical species,

sometimes during the course of the project. The data access screen forms for chemical species and phases, with the validation subroutines behind them, facilitate much of this tedious work.

A simple graphical presentation module in GEMS is very helpful in sampling selected modelling results, and presenting them as multiple plots (Fig. 2). The user defines what to sample, and how to re-calculate, by writing basic “math scripts”, which are automatically translated and executed. The sampled data can be exported as ASCII files of any format with the help of “printing scripts”. An on-line screenshot tutorial helps users learn how to operate GEMS for real modelling examples in a few hours. GEMS stores any modelling exercise in a separate “modelling project” directory, which can be zipped and shared with other users, or sent to the development team if something went wrong.

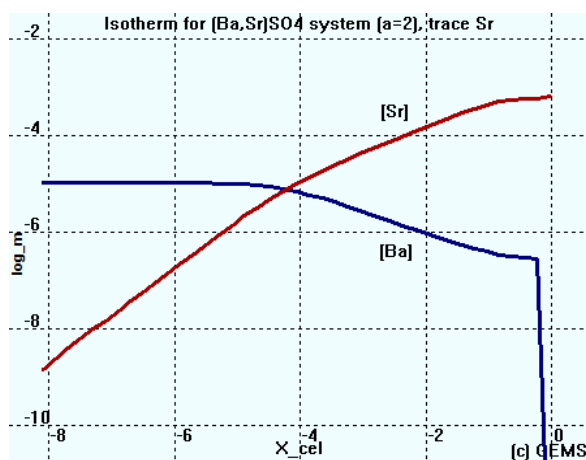


**Fig. 2:** Screen image of graphical output from GEMS “process simulation” of Sr isotherm in barite at  $P=1$  bar,  $T=25$  C. The ordinate “log\_m” is the logarithm of the total dissolved molality [M], and the abscissa “X\_cel” is the logarithm of the mole fraction of the celestite ( $\text{SrSO}_4$ ) end-member in a  $(\text{Ba,Sr})\text{SO}_4$  regular binary solid solution with the Margules parameter  $a=2$ .

Of course, user-friendliness alone cannot replace scientific efficiency in the GEM method, a point which is illustrated below in terms of two examples from our own usage of the code. Example 1 illustrates the prediction capabilities of solid-solution aqueous-solution models in applications relevant to nuclear waste disposal. Example 2 demonstrates how GEMS-PSI and DualTh calculations can be used in the interpretation of three independent experimental partitioning data sets. This leads to a new thermodynamic solid-solution aqueous-solution model of europium incorporation in calcite, applicable for a wide range of compositions at ambient temperatures. Another example of the power of GEM-Selektor in modelling a complex, redox-sensitive, solid-solution aqueous-solution hydro-thermal system can be found in a recent PSI Report

[21]. More applications of GEMS are currently in progress.

## 5 EXAMPLE 1: PREDICTING IMPROVED RETENTION OF RADIUM IN A NUCLEAR WASTE REPOSITORY

### 5.1 Background and Aims

Safety analysis studies for the Swiss High/Intermediate Level Waste (HLW/ILW) repository have clearly demonstrated that, in specific scenarios, the expected maximum concentration of  $^{226}\text{Ra}$  might become a critical issue. This is particularly true when the "classical" approach, which relies on solubility control by pure solid phases, is used to evaluate maximum dissolved nuclide concentrations. The example here presents this "classical" approach in the context of the repository chemical system sketched in Fig. 3.

Dissolved radium concentrations may be strongly affected by co-precipitation with barium and strontium sulphate minerals, c.f. [22], which are present as impurities in the repository backfill and host rock. Based on the more detailed inventory analysis, a simple solid-solution-based model accounting for this effect has been proposed and evaluated using GEMS [23]. In this way, the beneficial impact of the barium sulphate inventory on dissolved radium concentrations has been demonstrated.

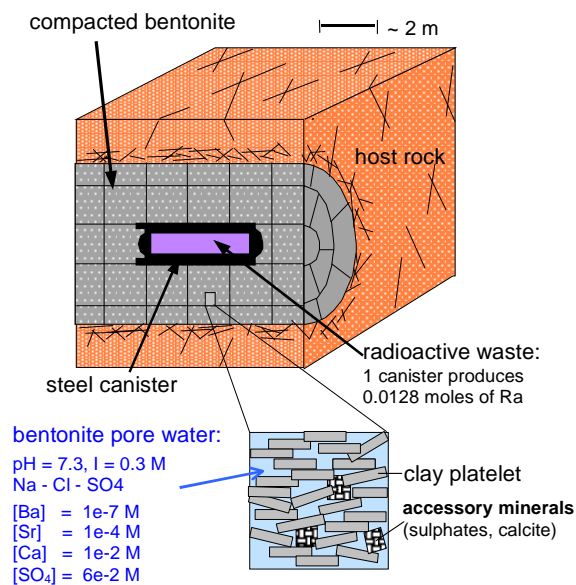


**Fig. 3:** Schematic of the repository (chemical) system addressed in Example 1. Properties of the pore water relevant to the study are given in the lower left corner.

### 5.2 "Classical" Solubility Calculation for Ra

The "classical" approach assumes that the total dissolved concentration of radium  $[\text{Ra}]_{\text{AQ}}$  is defined by an equilibrium with the least soluble pure Ra solid. A simple operational method has been adopted to calculate this solubility, starting from a pore solution

in equilibrium with compacted bentonite, the backfill material for the planned Swiss repository (brief indications are given in Fig. 3, and more details are provided in [24]). In our model, an increasing amount of  $\text{RaCl}_2$  "spike" is "added" to the pore-water/bentonite system. The radium solubility limit is attained when, according to the contents of the thermodynamic database, saturation with the most stable (i.e. least soluble) Ra solid has been established. Since the reference solution itself does not change to any significant degree, this procedure is the method of choice when trace concentrations are involved. In our specific bentonite pore water, the solid  $\text{RaSO}_4$  starts precipitating when the "added"  $[\text{RaCl}_2]_{\text{AQ}}$  reaches  $4.8 \cdot 10^{-8} \text{ M}$  ( $\text{mol} \cdot \text{L}^{-1}$ ). Thus, the solubility limit of Ra in the reference bentonite pore water is just  $4.8 \cdot 10^{-8} \text{ M}$ .

The distribution of Ra species in solution (i.e. the speciation) is dominated by the mono-sulphate complex and the free aqueous ion, plus a few percent of the mono-chloride complex:

$\text{RaSO}_4(\text{aq})$ :	$3.1 \cdot 10^{-8} \text{ M}$
$\text{Ra}^{2+}$ :	$1.6 \cdot 10^{-8} \text{ M}$
$\text{RaCl}^+$ :	$4.8 \cdot 10^{-10} \text{ M}$

This calculated maximum concentration is inversely proportional to the sulphate ion concentration (about 60 mM), and may thus be affected by all the variables which influence  $[\text{SO}_4^{2-}]_{\text{AQ}}$ : e.g. basic system definition, gypsum formation, sulphate reduction, etc. Up to this point, the conventional LMA geochemical speciation codes (Sec. 2.1) are sufficient (and well suited) to perform all calculations. The GEMS code performs similarly.

### 5.3 Model Concepts and Material Balances

In order to establish a solid solution model for predicting the behaviour of radium, it is essential to evaluate the detailed material balances in the system. Each waste canister, which contains the reprocessed waste of 1.8 tons of  $\text{UO}_2$  spent fuel, produces a maximum inventory of 0.0128 moles of  $^{226}\text{Ra}$  within 300 000 years after discharge from the reactor (cf. [25]). According to present layouts, each canister is surrounded on average by 57.4 tons of (dry) bentonite and 12.7 tons of pore solution.

The basic ideas for establishing a solid solution model from these facts are rather simple.

- The chemical behaviour of Ra is strongly related to that of Ba and Sr, due to well-established similarities in the chemical properties of these elements.
- The bentonite surrounding the waste contains minor impurities of Ba (and Sr) sulphates. However, compared to Ra, these impurities represent large quantities, considering there is 57.4 tons of bentonite. Further details may be taken from [23].

- In consequence of a very slow fluid motion through compacted bentonite, the chemical system has sufficient time to re-equilibrate (of the order of  $10^5$  years).

The radium mobilised from the waste (canister) is expected to interact with the barium/strontium sulphates (barite/celestite), present in the bentonite as impurities. Thus, radium is assumed to form a solid solution via re-crystallisation of the sulphates. This view is corroborated by the fact that pore waters of Opalinus Clay formations (the present host rock candidate for a Swiss repository) are saturated with respect to barite and celestite.

**Table 1:** Bulk composition recipe (in moles, water in kilograms) of a simplified chemical system. The resulting equilibrium solution is a Na-Cl-SO<sub>4</sub>-type water of pH 7.3. Its salt concentration corresponds to about half of sea-water salinity.

RaSO <sub>4</sub>	0.0128
BaSO <sub>4</sub>	71.86
SrSO <sub>4</sub>	38.22
Water	12740 kg
NaCl	2138.5
CaCO <sub>3</sub>	8025
CaSO <sub>4</sub>	796.8
Na <sub>2</sub> SO <sub>4</sub>	672.4
H <sub>2</sub> SO <sub>4</sub>	254.8
Air <sup>1)</sup>	large excess

<sup>1</sup>A large amount of artificial "dry air", including 0.63 mol% of CO<sub>2</sub>(g), 80 mol% of N<sub>2</sub>(g) and 19.4 mol% of O<sub>2</sub>(g), giving a CO<sub>2</sub> partial pressure of  $\log_{10}p_{\text{CO}_2} = -2.2$ .

Detailed inventories have been derived from trace element analyses of bentonites, and from the bentonite pore water composition [23,24]. A chemical system normalised to one waste canister has been constructed, as outlined in Table 1.

#### 5.4 Results of GEMS Solid Solution Modelling

In order to obtain a point of reference, the chemical system from Table 1 was first examined assuming that no solid solution is formed at all. As expected, the GEMS calculation yielded the same results as those previously obtained with the LMA code. A closer look at the earth-alkali-sulphate system shown in Table 2 reveals that all four sulphates co-exist at equilibrium, and that  $[\text{Ra}]_{\text{AQ}} = 4.8 \cdot 10^{-8} \text{ mol} \cdot (\text{kg H}_2\text{O})^{-1}$ , as before. Following the outline given above, in the next step it was assumed that BaSO<sub>4</sub>(s) and RaSO<sub>4</sub>(s) form an ideal solid solution. Table 3 demonstrates the dramatic impact of solid-solution partitioning on the dissolved Ra concentration.

Since RaSO<sub>4</sub>(s) and BaSO<sub>4</sub>(s) have nearly identical structures, and BaSO<sub>4</sub>(s) is present to large excess (i.e. 5641:1), the ideal mixing reduces dissolved Ra by about the same ratio: from  $4.8 \cdot 10^{-8}$  to  $8.6 \cdot 10^{-12}$  molal. The solubility of BaSO<sub>4</sub>(s), the "excess partner", is not changed to any significant degree.

Furthermore, using the capabilities of GEMS, we could easily evaluate the consequences of an ideal ternary solid solution, including SrSO<sub>4</sub>(s) as an additional end-member. In this case, we would predict  $[\text{Ra}]_{\text{AQ}}$  to decrease to  $5.6 \cdot 10^{-12}$  molal.

**Table 2:** GEMS calculation for the simplified chemical system given in Table 1, for convenience scaled down to 1 kg of water.

Amounts of solid at equilibrium			Solution
	[ $\mu\text{mol}$ ]		[ $\mu\text{mol} \cdot (\text{kg H}_2\text{O})^{-1}$ ] <sup>1)</sup>
RaSO <sub>4</sub>	0.956	<b>pure phase</b>	$[\text{Ra}]_{\text{AQ}}$ : <b>0.0483</b>
BaSO <sub>4</sub>	5640	pure phase	$[\text{Ba}]_{\text{AQ}}$ : 0.0889
SrSO <sub>4</sub>	2886	pure phase	$[\text{Sr}]_{\text{AQ}}$ : 114
CaSO <sub>4</sub>	70012	pure phase	$[\text{Ca}]_{\text{AQ}}$ : 13'826
			$[\text{SO}_4^{2-}]_{\text{AQ}}$ : 65'432

<sup>1</sup>A 0.3 % molality / molarity ( $\text{mol} \cdot (\text{kg of H}_2\text{O})^{-1}$  /  $\text{mol} \cdot \text{L}^{-1}$ ) difference was neglected.

It is known that miscibility in the (Sr,Ba)SO<sub>4</sub> solid solution series is rather limited [3], due to the different ionic radii of Sr<sup>2+</sup> and Ba<sup>2+</sup>. As the ionic radii of Ba<sup>2+</sup> and Ra<sup>2+</sup> are similar, the series (Sr,Ra)SO<sub>4</sub> should also have a large miscibility gap at room temperature. Hence, a model with two co-existing, binary solid solutions — ideal (Ba,Ra)SO<sub>4</sub>, non-ideal (Sr,Ra)SO<sub>4</sub> — appears to be more realistic than that with the ideal ternary solid solution (Ba,Sr,Ra)SO<sub>4</sub>.

**Table 3:** GEMS calculation for the simplified chemical given in Table 1, assuming BaSO<sub>4</sub>(s) and RaSO<sub>4</sub>(s) form an ideal solid solution.

Amounts of solid at equilibrium			Solution
	[ $\mu\text{mol}$ ]		[ $\mu\text{mol} \cdot (\text{kg H}_2\text{O})^{-1}$ ]
RaSO <sub>4</sub>	1.0	<b>end-member</b>	$[\text{Ra}]_{\text{AQ}}$ : <b>0.000086</b>
BaSO <sub>4</sub>	5640	<b>end-member</b>	$[\text{Ba}]_{\text{AQ}}$ : 0.0889
SrSO <sub>4</sub>	2886	pure phase	$[\text{Sr}]_{\text{AQ}}$ : 114
CaSO <sub>4</sub>	70 016	pure phase	$[\text{Ca}]_{\text{AQ}}$ : 13 823
			$[\text{SO}_4^{2-}]_{\text{AQ}}$ : 65 417

Some output from a single GEMS calculation, for a system with both (Ba,Ra)SO<sub>4</sub> and (Sr,Ra)SO<sub>4</sub> solid solutions, is shown in Figs. 4 and 5. The resulting  $[\text{Ra}]_{\text{AQ}} \sim 8.2 \cdot 10^{-12}$  molal is almost the same as that given in Table 3, where only the (Ba,Ra)SO<sub>4</sub> phase was involved. Therefore, radium is strongly partitioned towards barium sulphate, and the presence of the more soluble celestite plays no important role. Radium is not expected to partition into the more abundant, but more soluble, gypsum (CaSO<sub>4</sub>·2H<sub>2</sub>O; 70016  $\mu\text{mol} \cdot (\text{kg H}_2\text{O})^{-1}$  present). In the bentonite environment, the excess gypsum maintains a rather high total dissolved concentration of sulphate ( $[\text{SO}_4^{2-}]_{\text{AQ}} \sim 0.066$  molal, Fig. 4), which suppresses those of  $[\text{Ba}]_{\text{AQ}}$ ,  $[\text{Sr}]_{\text{AQ}}$  and  $[\text{Ra}]_{\text{AQ}}$ . Gypsum may be completely leached out of the system on a relatively short time-scale; in this scenario, a corresponding drop in  $[\text{S}]_{\text{AQ}}$  to 0.004 molal would increase  $[\text{Ra}]_{\text{AQ}}$  by 5-7 times only.

ICnam	b	Cb	u	lgm_t	m_t	ICnam
Ba	0.0071860001	5.3050886e-11	-306.1789	-7.0511773	8.8883817e-08	Ba
C	3.5854626	1.4132417e-10	-162.51103	-2.5528622	0.0027998697	C
Ca	0.82217998	1.3387905e-11	-290.52843	-1.8594084	0.01382266	Ca
Cl	0.21385	-4.0245585e-15	-24.376264	-0.77410948	0.16822499	Cl
H	141.4863	1.4474033e-11	-47.432843	-2.5905375	0.0025672164	H
Na	0.34833	5.0348614e-14	-138.01795	-0.56222784	0.27401362	Na
Nit	705.66403	2.2737968e-13	-0.11159832	-2.9871624	0.001030001	Nit
O	250.27481	2.9807187e-10	-0.82077567	-0.56733905	0.27080767	O
Ra	1.2800001e-06	7.8011412e-12	-315.81385	-11.086026	8.2030246e-12	Ra
S	0.18340928	5.8577421e-11	-240.02093	-1.1835634	0.06552946	S
Sr	0.0038220001	2.3680673e-11	-299.72361	-3.942556	0.00011414162	Sr
Zz	0	-1.1872383e-14	30.707211	-14.031209	9.3066029e-15	Zz

m\_t [8,0] : Output total dissolved molalities of Independent Components at equilibrium state

**Fig. 4:** A GEMS screen image, with results for ICs. Column “b” is the input bulk composition of the system (moles); “Cb” are the mass-balance residuals (moles); “u” are the dual solution potentials  $u_j$  (dimensionless); “m\_t” are total dissolved molalities of the ICs, and the “lgm\_t” are their decimal logarithms.

## 5.5 Discussion

Figure 5 shows in detail how radium is partitioned among the several solution phases.

In this calculation, the aqueous electrolyte, the gas mixture, the 3 solid solutions, and the 9 single-component solid phases, were all initially included.

At equilibrium, 6 phases were all found to be stable, including (Ba,Ra)SO<sub>4</sub> and (Sr,Ra)SO<sub>4</sub> solid solutions, calcite and gypsum. The pure Ra-sulphate phase is 3.77 orders of magnitude undersaturated. The (Ba,Ra)CO<sub>3</sub> phase is quite unstable in the presence of the sulphates.

Figure 6 outlines the impact of solid solution formation on trace element solubilities. The strong decrease in the trace element concentration is primarily an effect of end-member mole fractions, once the solid solution phase is stable. The properties of mixing and “common-anion” effects play a rather minor role at trace concentrations, as exemplified by the uncertainty band in Fig. 6

Unfortunately, *ideal* solid solution formation is by no means the rule; usually, *non-ideal* solid solutions, with narrow regions of mixing and miscibility gaps, are formed, but better knowledge of their thermodynamic properties is largely absent. However, at trace mole fractions, the non-ideality is sufficiently well approximated by assuming ideal behaviour, and by taking the stability of the trace end-member as  $G_{Tr}^* = G_{Tr}^o + \overline{G}_{Tr}^{Ex}$ .

Phase/species name	L	Type	x (moles)	log(activity)	Concentration	ln(gamma)
<b>Equilibrium</b>						
a aq_gen	45	a	71.203406			
g gas_gen	6	g	441.06262			
s [Ba,Ra]CO3[id]	2	s	0			
witherite		I	0	-5.3150648	0	0
RaCO3		I	0	-9.6366554	0	0
s [Ba,Ra]SO4[id]	2	s	0.0071871069			
barite		I	0.007185887	-7.3719393e-05	0.99983027	0
RaSO4		I	1.2198556e-06	-3.770244	0.00016972832	0
s [Sr,Ra]SO4[reg]	2	s	0.0036769618			
celestite		M	0.0036769017	-7.4039369e-06	0.99998365	6.2569898e-10
RaSO4		J	6.0126221e-08	-3.770244	1.6352147e-05	2.3399235
s Graphite	1	s	0			
s Calcite	1	s	0.77536519			
s Portlandite	1	s	0			
s Anhydrite	1	s	0			
s Gypsum	1	s	0.089243233			
gypsum		O	0.089243233	-2.5100446e-06	1	0
s Ra-carbonate	1	s	0			
s Ra-sulfate	1	s	0			
RaSO4		O	0	-3.770244	1	0
s Sulphur	1	s	0			
s Strontianite	1	s	0			
strontianite		O	0	-1.2676086	1	0

System: T = 298.15 K; P = 1.00 bar; V = 1.094e+04 L; Aqueous: built-in Davies; pH = 7.268; pe = 13.336; IS = 0.328 m

**Fig. 5:** Screen image of GEMS “System” dialogue showing the calculated equilibrium state. Note that more than 95% of radium is partitioned into the barite (“x (moles)” column). Activities of RaSO<sub>4</sub> species (“log(activity)” column) are equal in both solid solutions containing it, but the concentrations are *not* equal because of the different stabilities of the major end-members, and the different activity coefficients.

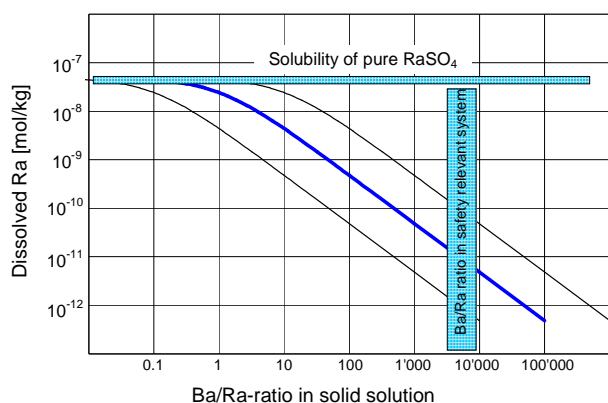


**Fig. 6:** The impact of  $(\text{Ba,Ra})\text{SO}_4$  solid solution on dissolved  $[\text{Ra}]_{\text{Aq}}$  as a function of available Ba inventory (thick solid curve). Thin solid curves reflect the solid solution stability uncertainties of one order of magnitude. The horizontal bar describes a “classical” situation, in which  $[\text{Ra}]_{\text{Aq}}$  is controlled by a pure  $\text{RaSO}_4$  phase.

## 6 EXAMPLE 2: EUROPIUM INCORPORATION IN CALCITE

### 6.1 Background

Trivalent europium,  $\text{Eu}^{\text{III}}$ , is a lanthanide element frequently used in laboratory studies as an analogue to  $\text{Am}^{\text{III}}$ ,  $\text{Cm}^{\text{III}}$  and  $\text{Pu}^{\text{III}}$ , three safety-relevant actinides occurring in various types of radioactive waste. In a long-term repository, these actinides will be leached from the waste matrix in trace concentrations, and will interact with the surrounding materials (e.g. cement and bentonite backfill). The main secondary product of cement alteration is calcite ( $\text{CaCO}_3$ ), a common reactive mineral hosting a variety of trace elements through solid solution formation [26]. Calcite is also present as a minor phase in Opalinus Clay, the host rock for the planned HLW/LW repository in Switzerland. The interaction of trace actinides with calcite rapidly produces dilute solid solutions, either through co-precipitation from an oversaturated solution, or through re-crystallisation of pre-existing calcite.

Many studies of calcite solid solutions have been published. Yet, the great majority are empirical ( $K_d$  determinations), and focus on the incorporation of divalent ions (e.g.  $\text{Cd}^{2+}$ ,  $\text{Mg}^{2+}$ ,  $\text{Sr}^{2+}$ ,  $\text{Ba}^{2+}$ ). Because these ions substitute for the equally charged  $\text{Ca}^{2+}$  (a *homovalent* substitution), the choice of end-member stoichiometry and structure is rather straightforward. Usually, such divalent metals form pure carbonates, with the same stoichiometry and structure as calcite ( $\text{CdCO}_3$ ,  $\text{MgCO}_3$ , etc.). Hence, the corresponding solid solution end-members can be easily defined. Because the solubility products,  $K_s^o$ , of these pure carbonates have been measured rather accurately, the standard free energy of formation of any divalent metal carbonate end-member,  $G_f^o(em)$ , can be easily calculated through the relations

$$\Delta G_R^0 = -RT \ln K_s^0 \quad (11)$$

$$\Delta G_R^0 = \sum \nu_p G_f^0(p) - \sum \nu_r G_f^0(r) - G_f^0(em) \quad (12)$$

where  $\Delta G_R^0$  is the standard molar free energy of the end-member dissolution reaction,  $G_f^0(r)$  and  $G_f^0(p)$  are the free energies of formation of auxiliary reactant and product species, the  $\nu_{p,r}$  are stoichiometry coefficients, and  $G_f^0(em)$  is the free energy of formation of the solid solution end-member to be determined. Once  $G_f^0(em)$  is known, binary solid solution models can be developed and compared against experimentally determined trace-metal solubilities.

The situation is far more complex for substituting ions such as  $\text{Eu}^{3+}$ , which have a different charge to that of  $\text{Ca}^{2+}$  (a *heterovalent* substitution). In this case, no obvious end-member stoichiometry can be defined, since formulae and structures of pure Eu-solids do not have much in common with calcite. Moreover, substitution of a trivalent cation for  $\text{Ca}^{2+}$  induces a local charge imbalance in the calcite structure, which must be compensated. The situation is made more complicated by the fact that different charge compensation mechanisms exist: for instance, a coupled substitution ( $\text{Na}^+ + \text{Eu}^{3+}$  for  $2 \text{Ca}^{2+}$ ), or a substitution of electro-neutral complexes ( $\text{Eu}(\text{OH})_3$  for  $\text{CaCO}_3$ ).

In this example, we show how the GEM method has been applied to develop an appropriate solid solution model, capable of explaining a large variety of experimental data on co-precipitated or recrystallised Eu calcites, obtained under widely different pH and  $\text{pCO}_2$  conditions [27]. In order to test the model, we considered three sets of data: (1) co-precipitation experiments at  $\text{pH} \sim 6$  and  $\text{pCO}_2 = 1$  bar, obtained in  $\text{Na-Ca-HCO}_3\text{-ClO}_4$  solutions of about 0.1 M electrolyte concentration [28]; (2) co-precipitation tests in synthetic seawater at  $\text{pH} \sim 8$  and  $\text{pCO}_2 = 0.0003 \div 0.3$  bar [29]; and (3) re-crystallisation tests in cement pore water at  $\text{pH} \sim 13$  and very low  $\text{pCO}_2$  [30].

### 6.2 Forward Binary Models

At the first modelling step, we applied a method very similar to that used for divalent cations. Four Eu solids exist, with well-known solubility products, from which the standard molar Gibbs free energy of formation for the corresponding Eu end-members can be derived.

As evident from Table 4, the free energy of the major end-member,  $\text{Ca}_n(\text{CO}_3)_n$ , must be scaled to the stoichiometric factor  $n = 1, 2$  or  $3$ . Each of the listed end-member pairs can be connected to a specific substitution mechanism. For instance, the  $\text{EuNa}(\text{CO}_3)_2\text{—Ca}_2(\text{CO}_3)_2$  solid solution implies a coupled substitution  $\text{Na}^+ + \text{Eu}^{3+} = 2 \text{Ca}^{2+}$ , while the  $\text{Eu}_2(\text{CO}_3)_3\text{—Ca}_3(\text{CO}_3)_3$  model implies that two of the three adjacent Ca-sites in calcite are substituted, but that the third one remains vacant.

**Table 4:** End-members and Gibbs free energies of formation ( $\text{kJ}\cdot\text{mol}^{-1}$ ) for the “forward” binary Eu-calcite solid solution models.

Europium side	$G_f^o$	Calcium side	$G_f^o$
$\text{Eu}_2(\text{CO}_3)_3$	-2932.7	$\text{Ca}_3(\text{CO}_3)_3$	-3387.6
$\text{EuOHCO}_3$	-1383.6	$\text{CaCO}_3$	-1129.2
$\text{EuNa}(\text{CO}_3)_2$	-2009.2	$\text{Ca}_2(\text{CO}_3)_2$	-2258.4
$\text{Eu}(\text{OH})_3$	-1201.0	$\text{CaCO}_3$	-1129.2

For the end-member pairs listed in Table 4, four ideal binary solid solution models were developed for the conditions relevant to the selected data. This means that four series of model calculations were performed for each of the three data sets. In each series, the overall equilibrium between the aqueous solution and the binary calcite solid solution was calculated for different total amounts of Eu in the system, yielding Eu equilibrium concentrations in the aqueous solution as functions of Eu mole fraction in calcite (*isotherms*). For instance, Fig. 7 shows isotherms resulting for the pH~6 data.

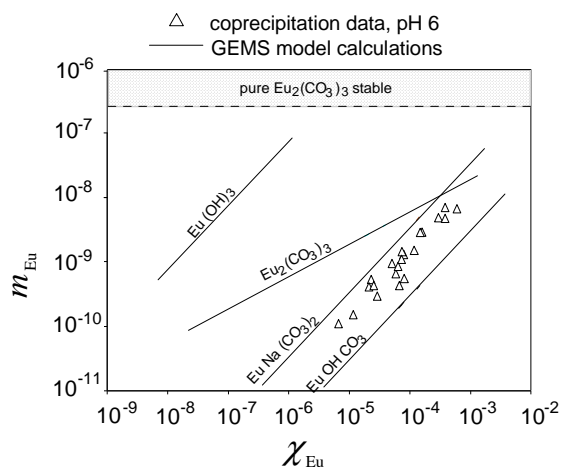


**Fig. 7:** Isotherms (lines) for binary Eu-calcite ideal solid solutions (Table 4), compared against the co-precipitation data [28] obtained at pH~6. The symbol  $\chi_{\text{Eu}}$  is the Eu mole fraction in calcite, and  $m_{\text{Eu}}$  is the equilibrium molality in aqueous solution.

These results demonstrate that binary solid solutions involving  $\text{Eu}_2(\text{CO}_3)_3$  or  $\text{Eu}(\text{OH})_3$  end-members must be rejected. The  $\text{Eu}_2(\text{CO}_3)_3$  end-member must be excluded because the slope defined by the model isotherm (+1/2) is not compatible with the trend defined by the experimental data (slope +1). The isotherm slope is related to the stoichiometry of Eu in the substituted complex. The +1 slope defined by the data implies substitution of isolated Eu cations in calcite, and excludes substitution of dimeric Eu groups (two Eu ions in adjacent Ca sites), in which case, a slope of +1/2 would arise in the isotherm plot.

The  $\text{Eu}(\text{OH})_3$  end-member must also be ruled out because of the too large discrepancy between model and data (non-ideality corrections can account for a shift of, at most, one order of magnitude). Finally, we also had to discard the  $\text{EuNa}(\text{CO}_3)_2$  end-member, because the experimental data do not show the expected sensitivity to dissolved  $[\text{Na}]_{\text{AQ}}$  concentrations. In conclusion, of the four binary models considered, only the  $\text{EuOHCO}_3$ – $\text{CaCO}_3$  solid solution is compatible with the data within a realistic non-ideal correction.

The same four binary models yielded surprisingly different results when applied to the other two experimental datasets [29,30] (not shown). It turned out that only a model involving  $\text{Eu}(\text{OH})_3$  would realistically explain the data obtained at pH~13, whereas the data obtained at pH~8 could be explained by assuming either  $\text{Eu}(\text{OH})_3$  or  $\text{Eu}_2(\text{CO}_3)_3$  as end-members.

### 6.3 DualTh Calculations and a Ternary Model

As a next step, we decided to test binary solid solutions with two additional hypothetical end-members,  $\text{EuH}(\text{CO}_3)_2$  and  $\text{EuO}(\text{CO}_3)_{0.5}$ , for which no pure solids (hence, no  $K_s^o$  or  $G_f^o$  values) are known.

We had to resort to an inverse modelling procedure, through which the standard Gibbs energy of formation  $G_f^o$  of a selected end-member is derived directly from the equilibrium partitioning data. From the results of the GEMS DualTh calculations (see Section 3.2), applied first to the equilibrated aqueous solutions, the chemical potentials of the proposed end-members were calculated at each single experimental point. With the help of the measured Eu mole fractions, free Gibbs energies of formation were then estimated. A given end-member was considered to be appropriate if almost the same  $G_f^o$  value resulted for all points of the experimental isotherm. In practice, a tolerance of  $\pm 2 \text{ kJ}\cdot\text{mol}^{-1}$  ( $\pm 0.35 \log K_s^o$ , units) was set for the standard deviation of the  $G_f^o$  estimates. The results of such calculations are presented in Table 5, for all six end-members considered so far.

**Table 5:** Mean end-member standard free energies of formation  $G_f^o$  ( $\text{kJ}\cdot\text{mol}^{-1}$ ) derived from DualTh calculations for the three considered datasets.

	pH~6	pH~8	pH~13
$\text{Eu}_2(\text{CO}_3)_3$	$-2939.9 \pm 4.6$	$-2921.8 \pm 1.4$	$-3106.6 \pm 6.0$
$\text{EuOHCO}_3$	$-1379.0 \pm 2.0$	$-1364.1 \pm 1.0$	$-1425.5 \pm 1.7$
$\text{EuNa}(\text{CO}_3)_2$	$-2010.2 \pm 2.3$	$-1994.5 \pm 1.0$	$-2088.8 \pm 1.7$
$\text{Eu}(\text{OH})_3$	$-1221.7 \pm 2.1$	<b><math>-1192.5 \pm 1.0</math></b>	<b><math>-1193.3 \pm 1.7</math></b>
$\text{EuH}(\text{CO}_3)_2$	<b><math>-1775.1 \pm 2.0</math></b>	<b><math>-1774.6 \pm 1.0</math></b>	$-1896.6 \pm 1.7$
$\text{EuO}(\text{CO}_3)_{0.5}$	$-1063.2 \pm 2.3$	$-1041.0 \pm 1.0$	$-1072.2 \pm 1.7$

Equivalent  $G_f^o$  values (shown in boldface in Table 5) result from two out of the three data sets, if either  $\text{Eu}(\text{OH})_3$  or  $\text{EuH}(\text{CO}_3)_2$  is assumed as a minor end-member of the binary solid solution. This means that all three sets of experimental data cannot be described simultaneously by any binary model. However, assuming a *ternary* solid solution  $\text{EuH}(\text{CO}_3)_2$ - $\text{Eu}(\text{OH})_3$ - $\text{CaCO}_3$ , with free energies of Eu end-members as specified in boldface in Table 5, a consistent model for all three experimental data sets can be constructed. We have tested this hypothesis, and obtained the results plotted in Fig. 8.

Indeed, all three datasets could be reproduced simultaneously on the basis of the above-mentioned ideal ternary solid solution model. The content of Eu in the solid solution phase is strongly dominated by the  $\text{EuH}(\text{CO}_3)_2$  end-member in the pH-6 calcites, and by the  $\text{Eu}(\text{OH})_3$  end-member in the pH-13 calcites. *Both* Eu end-members are present in comparable mole fractions in the pH-8 calcites. Moreover, we were able to show that ternary solid-solution models, involving any other pair among the six Eu end-members listed in Table 5, fail to explain all the data, regardless of the assumed  $G_f^o$  values.

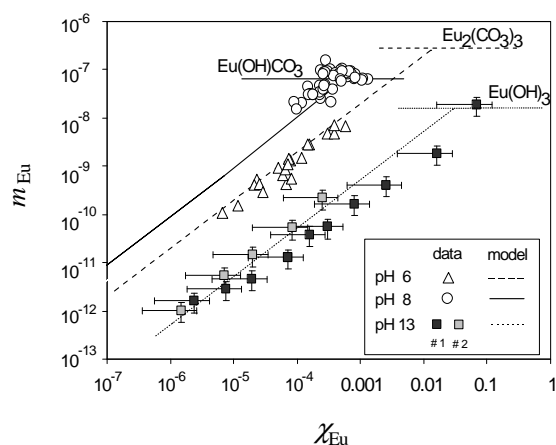


**Fig. 8:** Experimental results (symbols) compared with predicted isotherms (lines) based on the same ternary  $\text{EuH}(\text{CO}_3)_2$  –  $\text{Eu}(\text{OH})_3$  –  $\text{CaCO}_3$  ideal solid solution model. Horizontal lines define the solubility limits set by pure Eu-solids under the relevant experimental conditions.

In conclusion, the GEM thermodynamic calculations we have performed suggest that heterovalent carbonate solid solutions are complex, and may involve incorporation of multiple trace-metal species. The identification of appropriate end-members is not trivial, and requires, firstly, extensive partitioning solubility data to be obtained, which should then be processed using the GEM DualTh technique, and, secondly, be supported by spectroscopic evidence.

In this particular case, our ternary solid solution model is corroborated by independent laser fluorescence data [31], indicating the existence of two independent  $\text{Eu}^{\text{III}}$  species in calcite, one being partially hydrated.

## 7 ON-GOING AND FUTURE DEVELOPMENTS

Continuous development and support of the GEMS-PSI code is aimed at improving quality and performance, first of all by adding the new functionality important for performance assessment of nuclear waste repositories. At the same time, this improvement will be of benefit for a growing scientific community of GEMS users. Notwithstanding the routine IT-engineering tasks (aimed at optimising researchers' working time), three lines of development, considered to be important in the near future, should be mentioned. These are itemised in the sub-sections below.

### 7.1 Sorption Continuum and the DualTh Module

The GEMS-PSI code offers two alternative approaches for the thermodynamic modelling of the uptake by mineral solids of dissolved elements: the surface complexation models (SCM) [14,32], and the solid-solution aqueous-solution (SSAS) models (see examples above). Taken together or alone, these approaches can generate "smart  $K_d$ " values, by modelling the whole "sorption continuum" (from adsorption to solid solution) in elemental stoichiometry only, without additional balance constraints for surface sites. This strategy can help in the prediction of stability of clay minerals, and the radionuclide sorption in them, over long time-scales [33]. It also opens a way towards future development of a uniform chemical thermodynamic database for (trace) element sorption [32] as a consistent extension of the existing databases for aqueous species, gases and minerals.

The DualTh techniques (see Sections 3.2 and 6) can help considerably in interpreting  $K_d$  values from sorption experiments, in terms of standard thermodynamic properties of solid-solution end-members or surface complexes. Given that the  $\mathbf{u}$  vector is computed by GEMS from each experimental aqueous composition, the remaining calculations are simple, and can be performed using, for example, an Excel spreadsheet. However, this is a rather time-consuming process, because of the need to export GEM results and related thermodynamic data from the GEMS database to the spreadsheet, and then import the DualTh estimated values back into the GEMS modelling project, and the fact that the entire cycle is usually repeated several times.

Many of these tedious operations could be avoided if DualTh calculations were implemented as a separate module in the GEMS package, and as one having a direct access to the necessary parts of the project database. This would save up to 90% of the researcher's time now needed for preparing the DualTh spreadsheet. Thus, implementation of the *DualTh* module is a top priority task in the further development of the GEMS-PSI code.

## 7.2 Model Sensitivity and the *UnSpace* Module

In geochemical modelling, the input data are usually treated in a deterministic way, though, in reality, neither the thermodynamic data ( $G_{j,T}^o, \mathcal{H}_j$ ) nor the variables of state ( $\mathbf{b}, P, T$ ) are known precisely. Consequently, by taking all input data as deterministic, the modeller risks being led to wrong conclusions. When reasonable uncertainty intervals are available from analytical error estimates, or from a critical compilation of thermodynamic constants, the sensitivity and robustness of a particular geochemical model can be assessed using Monte Carlo simulations, which generate many (hundreds to thousands) of “sample calculations”, and treat them statistically.

We believe that the main difficulty in these kinds of studies lies in the interpretation of sampled output data. As shown by Karpov and his co-workers [34], for sufficiently large uncertainties in input data, the *a priori* correct result may not be the most frequent one among the generated sample variants.

To solve the problem, a new method has been proposed that involves: (i) the GEM IPM algorithm used for sampling the multi-dimensional “uncertainty space” over a uniform probing grid; and (ii) an advanced analysis, combining “dual thermodynamics” with the “decision-making” criteria projected from game theory. In a pilot study [35], performed in collaboration with Prof. Karpov’s group in Russia, the potential of this method has been explored. We have also found that independent experimental information can be used in combination with decision-making criteria to “filter” the “uncertainty space”. This helps in discarding unrealistic sample variants, which further reduces the initially-applied uncertainty intervals. We believe that, in this way, a much more robust interpretation of thermodynamic modelling results can be finally achieved.

The “uncertainty space” concept, as outlined above, opens an exciting research perspective. As a supporting tool for future model sensitivity studies, a new *UnSpace* module will be implemented into a forthcoming version of the GEMS-PSI code.

## 7.3 Coupling with Fluid-Mass-Transport Codes

Prediction of radionuclide migration implies simultaneous accounting of the diffusive/advective mass transport and the chemical interactions. The latter may cause dissolution/precipitation of the solid phases, which, in turn, may influence porosity, hydraulic conductivity and mass-transport pathways [36].

In principle, the calculation of equilibrium states in GEM proceeds without considering chemical reactions and depends only on changing the bulk composition  $\mathbf{b}$ ,  $T$  and  $P$  of the chemically reactive sub-system. Hence, it is possible to couple GEM with a fluid-mass-transport (FMT) algorithm in a “cleanly separated”, modular-based fashion; i.e. without

introducing any chemical mass-action terms into the mass-transport equations. In such coupling schemes, the FMT part should take care only of mass/heat conservation across the node borders, while the GEM algorithm would fully account for the local/partial equilibration in each nodal volume.

In the foreseen implementation, the first step would be to develop the necessary data structures for the information exchange between the FMT and GEM parts. The second step would then be to isolate the IPM-2 algorithm into a separate “kernel” module, which could communicate via those data structures with any FMT code (and with the GEMS-PSI GUI shell); the GEM IPM “kernel” module should also be able to run on parallel computers. Thus, with such a strategy implemented, it would be possible to produce a new generation of FMT-GEM coupled algorithms and codes for modelling, for example, near- and far-field repository systems, with the most extensive account being taken of the chemical interactions and induced FMT parameter changes.

## ACKNOWLEDGMENTS

We are greatly indebted to other members of GEMS-PSI development team: namely, K.V. Chudnenko, S.V. Dmitrieva, I.K. Karpov, A.V. Rysin, and T. Thoenen, who helped make the GEMS package a reality. The work presented in this article was funded in part by the Swiss National Cooperative for the Disposal of Radioactive Waste (NAGRA).

## REFERENCES

- [1] D.L. Parkhurst, C.A.J. Appelo, “*User’s guide to PHREEQC (Version 2) — A computer program for speciation, batch-reaction, one-dimensional transport, and inverse geochemical calculations*”. U.S.G.S. Water-Resources Investigations Report 99-4259, Denver, Colorado, 1999.
- [2] P.D. Glynn, “*MBSSAS: A computer code for the computation of Margules parameters and equilibrium relations in binary solid-solution aqueous-solution systems*”, *Comput. Geosci.*, **17**, 907-966 (1991).
- [3] P. Glynn, “*Solid solution solubilities and thermodynamics: sulfates, carbonates and halides*”, in: “*Sulfate minerals: Crystallography, geochemistry and environmental significance*”, eds. J.L. Jambor, D.K. Nordstrom, *Rev. Mineral. Geochem.*, **40**, 481-511 (2000).
- [4] D.A. Kulik, M. Kersten, U. Heiser, T. Neumann, “*Application of Gibbs energy minimization to model early-diagenetic solid-solution aqueous-solution equilibria involving authigenic rhodochrosites in anoxic Baltic Sea sediments*”, *Aquat. Geochem.*, **6**, 147-199 (2000).

- [5] J.C. Westall, J.L. Zachary, F.M.M. Morel, "MINEQL: A computer program for the calculation of chemical equilibrium composition of aqueous systems", Technical Note 18, Dept. of Civil Engineering, MIT, Cambridge, Massachusetts, 1976.
- [6] T.J. Wolery, "EQ3/6, A software package for geochemical modelling of aqueous systems: package overview and installation guide (V. 7.0)", [//geosciences.llnl.gov/esd/geochem/eq36.html](http://geosciences.llnl.gov/esd/geochem/eq36.html), LLNL UCRL-MA-110662 (1992).
- [7] C.W. Bale, P. Chartrand, S. A. Degterov, G. Eriksson, K. Hack, R. Ben Mahfoud, J. Melancon, A.D. Pelton, S. Petersen, "FactSage thermo-chemical software and databases", *Calphad* **26**, 189-228 (2002).
- [8] G. Eriksson, K. Hack, "Chemsage — A computer program for the calculation of complex chemical equilibria", *Metallurg. Transact. B*, **21**, 1013-1023 (1991).
- [9] M. V. Borisov, Yu.V. Shvarov, "Thermodynamics of geochemical processes", MSU Publ., Moscow, 1992 (in Russian).
- [10] I.K. Karpov, K.V. Chudnenko, D.A. Kulik, "Modelling chemical mass transfer in geochemical processes: thermodynamic relations, conditions of equilibria, and numerical algorithms", *Amer. J. Sci.*, **297**, 767-806 (1997).
- [11] I.K. Karpov, K.V. Chudnenko, D.A. Kulik, O.V. Avchenko, V.A. Bychinskii, "Minimization of Gibbs free energy in geochemical systems by convex programming", *Geochem. International*, **39**, 1108-1119 (2001).
- [12] C. Bethke, "Geochemical reaction modeling: concepts and applications", Oxford Univ. Press, New York, 1996.
- [13] F.M.M. Morel, J.G. Hering, "Principles and applications of aquatic chemistry", Wiley Interscience, New York, 1993.
- [14] D.A. Kulik, "Gibbs energy minimization approach to model sorption equilibria at the mineral-water interface: Thermodynamic relations for multi-site-surface complexation", *Amer. J. Sci.*, **302**, 227-279 (2002).
- [15] K.V. Chudnenko, I.K. Karpov, D.A. Kulik, "A high-precision IPM-2 minimization module of GEM-Selektor v.2-PSI program package for geochemical thermodynamic modelling", PSI Technical Report TM-44-02-06, Paul Scherrer Institute, Villigen, Switzerland, 2002.
- [16] D.A. Kulik, M. Kersten, "Aqueous solubility diagrams for cementitious waste stabilization systems. 4. A carbonation model for Zn-doped calcium silicate hydrate by Gibbs energy minimization", *Environ. Sci. Technol.*, **36**, 2926-2931 (2002).
- [17] J. Blanchette, M. Summerfield, "C++ GUI programming with Qt 3", Prentice Hall PTR, New Jersey (2004); also <http://www.trolltech.com>.
- [18] W. Hummel, U. Berner, E. Curti, F.J. Pearson, T. Thoenen, "Nagra/PSI Chemical Thermodynamic Database 01/01", Universal Publishers/ uPUBLISH.com, Parkland FL, 2002.
- [19] E.L. Shock, D.C. Sassani, M. Willis, D.A. Sverjensky, "Inorganic species in geologic fluids: correlations among standard molal thermodynamic properties of aqueous ions and hydroxide complexes", *Geochim. Cosmochim. Acta* **61**, 907-950 (1997); also [http://geopig.asu.edu/supcrt\\_data.html](http://geopig.asu.edu/supcrt_data.html).
- [20] T. Thoenen, D. Kulik, "Nagra/PSI chemical thermodynamic data base 01/01 for GEM-Selektor v.2-PSI modelling code: Release 28-02-03", PSI Technical Report TM-44-03-04, Paul Scherrer Institute, Villigen, Switzerland, 2003.
- [21] V.A. Kurepin, D.A. Kulik, A. Hiltbold, M. Nicolet, "Thermodynamic modelling of Fe-Cr-Ni spinel formation at the light-water reactor conditions", PSI Report 02-04, Paul Scherrer Institute, Villigen, Switzerland, 2002.
- [22] D. Langmuir, "Aqueous environmental geochemistry", Prentice Hall, New Jersey, 1997.
- [23] U. Berner, E. Curti, "Radium solubilities from SF/HLW wastes using solid solution and coprecipitation models", PSI Technical Report TM-44-02-04, Paul Scherrer Institute, Villigen, Switzerland, 2002.
- [24] E. Curti, P. Wersin, "Assessment of pore water chemistry in the bentonite buffer for the Swiss SF/HLW repository", Technical Report NTB 02-09, Nagra, Wettingen, Switzerland, 2002.
- [25] J.-Cl. Alder, D. McGinnes, "Model radioactive waste inventory for Swiss waste disposal projects", Technical Report NTB 93-21, Nagra, Wettingen, Switzerland, 1994.
- [26] E. Curti, "Coprecipitation of radionuclides with calcite: estimation of partition coefficients based on a review of laboratory investigations and geochemical data", *Appl. Geochem.*, **14**, 433-445 (1999).
- [27] E. Curti, D.A. Kulik, J. Tits, "Solid solutions of trace Eu(III) in calcite: thermodynamic evaluation of experimental data in a wide range of pH and pCO<sub>2</sub>", *Geochim. Cosmochim. Acta*, submitted (2004).
- [28] L.Z. Lakshatnov, S.L.S. Stipp, "Experimental study of Europium (III) coprecipitation with calcite", *Geochim. Cosmochim. Acta*, **68**, 819-827 (2004).

- [29] S. Zhong, A. Mucci, "Partitioning of rare earth elements (REEs) between calcite and seawater solutions at 25°C and 1 atm, and high dissolved REE concentrations", *Geochim. Cosmochim. Acta*, **59**, 443-453 (1995).
- [30] J. Tits, E. Wieland, M.H. Bradbury, P. Eckert, A. Schaible, "The uptake of Eu(III) and Th(IV) by calcite under hyperalkaline conditions", PSI Report 02-03, Paul Scherrer Institute, Villigen, Switzerland, 2003.
- [31] T. Stumpf, T. Fanghänel, "A time-resolved laser fluorescence spectroscopy (TRLFS) study of the interaction of trivalent actinides (Cm(III)) with calcite", *J. Colloid Interf. Sci.*, **249**, 119-122 (2002).
- [32] D.A. Kulik, "Sorption modelling by Gibbs energy minimisation: Towards a uniform thermodynamic database for surface complexes of radionuclides", *Radiochim. Acta*, **90**, 815-832 (2002).
- [33] D. Kulik, E. Curti, U. Berner, "Thermodynamic modelling of radionuclide retention on clays: surface complexation or solid solution equilibria?", in: *Clays in natural and engineering barriers for radioactive waste confinement* (ANDRA International Meeting, Reims, France, December 9-12, 2002), Abstract: O-5a-1 (oral), p.63-64 (2002).
- [34] I.K. Karpov, K.V. Chudnenko, M.V. Artimenko, V.A. Bychinski, D.A. Kulik, "Thermodynamic modelling of geological systems by convex programming under uncertainty", *Russ. Geol. Geophys.*, **40**, 971-988 (1999) (in Russian).
- [35] K.V. Chudnenko, I.K. Karpov, D.A. Kulik, U.R. Berner, W. Hummel, M.V. Artimenko, "GEM Uncertainty Space approach for sensitivity analysis of solid-aqueous chemical equilibrium models: a pilot study", PSI Technical Report TM-44-04-01, in preparation (2004).
- [36] W. Pfingsten, "Efficient modelling of reactive transport phenomena by a multispecies random walk coupled to chemical equilibrium", *Nuclear Technology*, **116**, 208-221 (1996).